Connected Variable Speed Limits Control and Vehicle Acceleration Control to Resolve Moving Jams

Meng Wang (corresponding author)
Delft University of Technology, Faculty of Civil Engineering and Geoscience
Stevinweg 1, 2628 CN Delft, The Netherlands
phone: +31 15 27 84030, fax: +31 15 27 83179
m.wang@tudelft.nl

Winnie Daamen
Delft University of Technology, Faculty of Civil Engineering and Geoscience
Stevinweg 1, 2628 CN Delft, The Netherlands
phone: +31 15 27 85927, fax: +31 15 27 83179
w.daamen@tudelft.nl

Serge P. Hoogendoorn
Delft University of Technology, Faculty of Civil Engineering and Geoscience
Stevinweg 1, 2628 CN Delft, The Netherlands
phone: +31 15 27 85475, fax: +31 15 27 83179
s.p.hoogendoorn@tudelft.nl

Bart van Arem
Delft University of Technology, Faculty of Civil Engineering and Geoscience
Stevinweg 1, 2628 CN Delft, The Netherlands
phone: +31 15 27 86342, fax: +31 15 27 83179
b.vanarem@tudelft.nl

Paper submitted to TRB Annual Meeting 2015
July 31, 2014
5677 words + 5 figure(s) + 2 table(s)

ABSTRACT

The vision of intelligent vehicles traveling in road networks has prompted numerous concepts to control future traffic flow, one of which is the in-vehicle actuation of traffic control signals. The key of this concept is using intelligent vehicles as actuators for traffic control systems, replacing the traditional road-side systems. Under this concept, we design and test a control system that connects a traffic controller with in-vehicle controllers with Vehicle-to-Infrastructure communications. The link-level traffic controller regulates traffic speeds through variable speed limits (VSL) gantries to resolve stop-and-go waves, while intelligent vehicles control accelerations through vehicle propulsion and brake systems to optimize their local situations. It is assumed that each intelligent vehicle receives VSL commands from the traffic controller and uses them as variable parameters for the local vehicle controller. Feasibility and effectiveness of the connected control paradigm are tested in simulation on a two-lane freeway stretch with intelligent vehicles randomly distributed among human-driven vehicles. Simulation shows that the connected VSL and vehicle control system improves traffic efficiency and sustainability, i.e. total time spent in the network and average fuel consumption rate are reduced compared to (uncontrolled and controlled) scenarios with 100% human drivers and to uncontrolled scenarios with the same intelligent vehicle penetration rates.

INTRODUCTION

Information and communication technologies enable cooperative vehicle infrastructure systems, where intelligent vehicles (IVs) connect with each other via vehicle-to-vehicle (V2V) communication and with road infrastructure via vehicle-to-infrastructure (V2I) communication. Numerous control concepts have been proposed during the past two decades with regard to traffic control systems with IVs, most of which pertain to a hierarchical structure where road-based traffic control systems are placed on top of vehicle control systems (*1, 2, 3, 4, 5, 6*). Based on the spatial and temporal scope of the considered control system, several control levels can be distinguished in the hierarchy, i.e. network, link, (platoon and) vehicle levels (*1, 7*). The works in (*1, 7*) provide a detailed description on the hierarchical architecture. In this paper, we focus on the connection between link-level controller and vehicle-level controller via V2I communications.

The potential of connected traffic control systems with IVs compared to the traditional traffic control systems is twofold. Firstly, with V2I communications, the traffic controller can get individual vehicle information from IV sensors to estimate the traffic state. The data from IVs are usually provided in a finer spatio-temporal resolution and better accuracy compared to road-based sensors (*8, 9, 10*). The second potential is the better actuation of traffic control commands, where IVs are used as actuators of road-based traffic control systems (*1, 4, 11*). The control signals are transmitted to the IVs via V2I communication, and the signals are used as commands for vehicle-level controllers, i.e. IVs are forced to execute the control commands from traffic control systems.

Next to these opportunities, road operators face some new challenges, one of which is that the resulting traffic flow characteristics may change substantially with IVs traveling in the network. In (*7*), it has been shown that the formation and propagation of moving jams (also called stop-and-go waves) with IVs are quite distinct to those with all human-driven vehicles. Hence, the question of whether the current active traffic management (ATM) measures based on human-driven vehicular flow phenomena still work well with IVs arises. The answer to this question is of great importance for road operators to develop ATM systems to control future traffic flow IVs.

This paper presents a proof-of-concept study for the connected link-level variable speed limits (VSL) control system with intelligent vehicles equipped with Car-Following Control (CFC) systems. The main objective is to examine the feasibility of the connected control paradigm and to identify the potential improvements in control effectiveness. A VSL control algorithm that is dedicated to resolve moving jams is employed as the link-level controller, while a CFC algorithm that controls vehicle accelerations based on model predictive control approach is developed and employed by the vehicle-level controller. The two-level controllers are connected via Dedicated Short Range Communications (DSRC). The connected control system is tested near a freeway bottleneck where CFC vehicles are randomly distributed in the network. Simulation experiments with different penetration rates of CFC vehicles in the network are conducted to test the change in flow characteristics and in control effectiveness.

In the sequel, we first describe the design and operation of the connected traffic and vehicle control system. Then the experimental design is presented. After that, the flow characteristics with IVs in uncontrolled scenarios (without VSL controller) are briefly discussed, followed by the test results of the scenarios with the connected control system. Conclusions and suggestions for future research directions are summarized in the end.

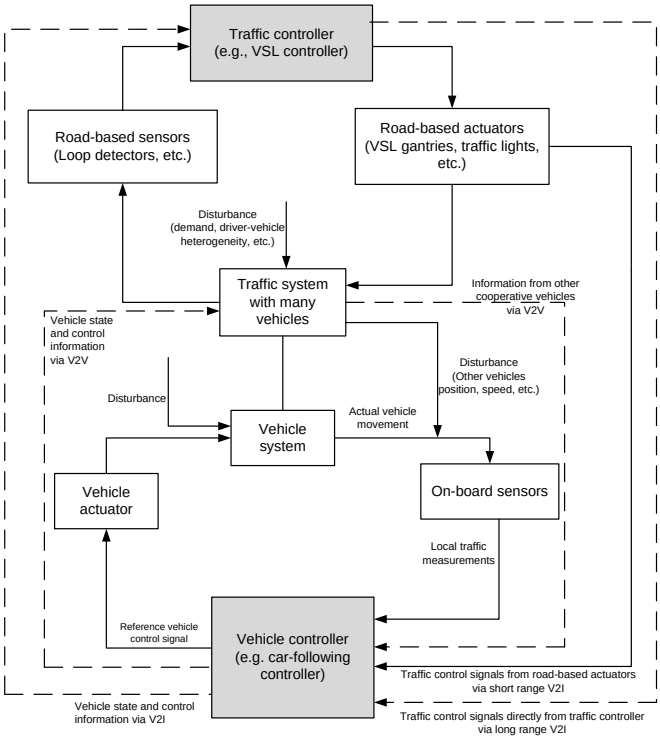

FIGURE 1 Schematic representation of the bi-level control problem. Dashed lines are not covered in this study.

CONTROL DESIGN OF CONNECTED TRAFFIC AND VEHICLE CONTROL SYSTEM

Figure 1 shows a schematic representation of the connected control concept, with arrows indicating the information flow. At the upper level, the traffic controller estimates the *freeway traffic state* of the road network based on measurements from road-based sensors and on information from IVs in the network via vehicle-to-infrastructure (V2I) communication, and generates traffic control signals, such as VSL. The traffic control signals are transmitted to and executed by road-based actuators, such as VSL gantries. The traffic control signal can also be transmitted directly to IVs from traffic controllers or from road-based actuators. As the vehicles in the network move based on the *local* interactions and the traffic control signals, the *freeway traffic state* changes, and the traffic controller enters the next control cycle, which is typically in the order of minutes.

At the lower level, the vehicle controller, such as the CFC controller, estimates the *local situation* surrounding the vehicle based on the measurements from on-board sensors. The traffic control commands from the traffic controller are used by the vehicle controller to compute the reference control signals, such as accelerations. The reference signal of the vehicle control system is executed by the vehicle actuators. The control cycle of the vehicle controller is typically in the order of less than one second. The state and control information of the vehicle controller may also be transmitted to the upper-level traffic controller via V2I communication, or to other vehicles via V2V communication, which is not the focus of this study.

The remaining of this section presents the assumptions regarding the operation of the connected control system, the algorithms at link and vehicle levels and the controller implementation in a microscopic simulation model.

Assumptions of Integrated Control System

The following assumptions are made for the operation of the connected VSL control with CFC system on a freeway stretch:

- There are loop detectors every 250 meters along the freeway, collecting aggregate flow and speed data every 30 seconds. VSL gantries are positioned every 500 meters along the freeway. Measurement errors from detectors are not considered in this study, but are addressed in another work (*12*).
- The VSL controller uses data from loop detectors to estimate and to predict the state of the traffic system on the freeway.
- The transmission of VSL signals from VSL gantries to CFC vehicles are via Dedicated short range communication (DSRC) (*11*). The DSRC range is 200 meters and the DSRC delay is negligible compared to the VSL control cycle.
- A CFC vehicle detects the gap and speed difference with respect to the predecessor solely based on its own on-board sensors, e.g. forward-looking radar. The CFC vehicle predicts the behavior of its predecessor and determines its optimal accelerations to minimize its objective function.
- CFC vehicles are assumed to fully comply with the speed limits, while human drivers do not fully comply. Under the speed limit of 60 km/h, human drivers are assumed to choose their desired speeds at 72 km/h, which is in accordance with field test results (*13*).

VSL Control Algorithm: SPECIALIST

At link level, a VSL control algorithm, namely SPECIALIST (SPEed ControllIng ALgorIthm using Shockwave Theory) (*13*), is chosen for this case study. Compared to other VSL control strategies (*14*, *15*), SPECIALIST algorithm is easy to tune and has been tested on a Dutch freeway (*13*). It is a feedforward controller and resolves moving jams based on shock wave theory (*16*).

Shock wave theory states that the wave front between two states in the left figure of Figure 2 has the same slope as that of the line that connects the two states in the fundamental diagram in the right figure of Figure 2. The approach to resolve stop-and-go waves consists of four phases and starts with a shock wave as shown in Figure 2.

Phase I. A shock wave (shown as state 2 in Figure 2) is detected on the freeway. We assume that the traffic state upstream (state 6) and downstream (state 1) of the shock wave is in free flow which is generally the case in real traffic. For illustration simplicity, we assume state 1 and 6 has the same state and density value. The theory holds when the two states are different (*13*).

Phase II. As soon as the shock wave is detected, the speed limits of (60 km/h) upstream of the shock wave are switched on. This leads to a state change in the speed-controlled area from state 6 to state 3, and to the boundary between areas 6 and 3. State 3 has the same density as state 6. However, the flow of state 3 is lower than that of state 6 due to the combination of the same density with a lower speed. The front between states 2 and 3 will propagate backwards with a lower speed than the front between states 1 and 2, and consequently the two fronts will intersect and the shock wave will be resolved after some time.

At the upstream end of the speed-limited area traffic will flow into this area, with the speed equaling the speed limit and with a density corresponding to the speed limit, typically significantly higher than the density of state 3. This forms state 4. The propagation direction of the front between states 6 and 4 depends on the flow of state 4.

Phase III. When the shock wave (area 2) is resolved, there remains an area with the speed

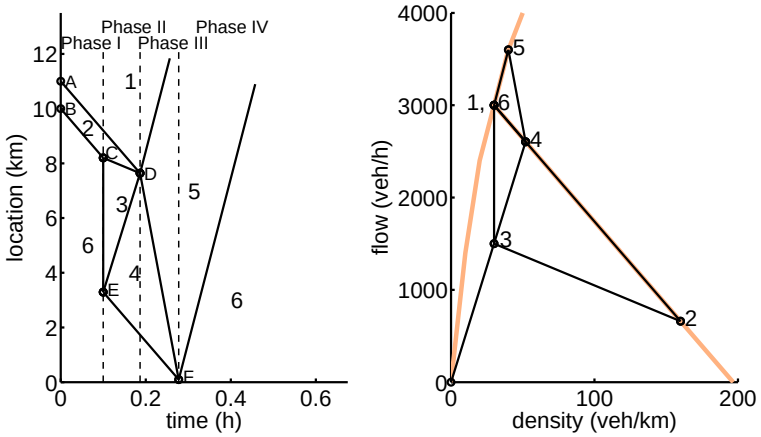

FIGURE 2 The four phases of the SPECIALIST algorithm, reproduced after (*12*). Flow and density values are for two lanes. The numbers denote different traffic states

limits active (state 4) with a moderate density (higher than in free-flow, but lower than in a shock wave) and a moderate speed. This theory postulates that the traffic from such an area can flow out more efficiently than a queue discharging from full congestion as in the shock wave. The traffic leaving area 4 will have a higher flow and a higher speed than state 4, represented by state 5. This leads to a backward propagating front between states 4 and 5, which resolves state 4.

Phase IV. The remaining states are areas 5, 6 and 1. The wave front between states 1 and 5, and that between states 6 and 5 both propagate downstream. In the end, the backward propagating shock wave is converted into a forward propagating wave.

Based on the theory, an algorithm is developed that is suited for real-world implementation. First, a shock wave is detected by using thresholds V_{max} (km/h) for the speed measurements, by assuming that in segment i, a shock wave is present if $V_i \leq V_{\text{max}}$. After that, traffic states 1-6 are determined using measurements from sensors and a control scheme is generated, involving the determination of the various fronts and their intersection points by solving linear equations based on the shock wave theory (*13*). After that the control scheme is determined and the speed limit can be activated. For details of the algorithm, we refer to (*13, 12*).

Car-Following Control Algorithm

In previous work, a CFC algorithm based model predictive control (MPC) approach is developed (*17*). The CFC system operates in two modes, being following mode and cruising mode. In cruising mode, the CFC controller minimizes driving efficiency and comfort costs, while in following mode it minimizes safety cost in addition to efficiency and comfort costs.

Let the system state $\mathbf{x}$ from the perspective of a CFC vehicle be described by the gap (or distance) s and relative speed $\Delta v = v_l - v$ to the predecessor, $\mathbf{x} = (s, \Delta v)^T$, where v and v_l denotes the speed of the CFC vehicle and that of its predecessor respectively. Let $\mathbf{u} = u$ denote the controlled acceleration. At each sampling time, the MPC CFC controller solves a finite horizon optimal control problem at current time $t = 0$ with initial state $\mathbf{x}(0) = \mathbf{x}_0$ as follows:

$$\min_{\mathbf{u}} J(\mathbf{x}, \mathbf{u}) = \min_{\mathbf{u}} \int_0^{T_P} \mathcal{L}(\mathbf{x}(\tau), \mathbf{u}(\tau)) \mathrm{d}\tau \tag{1}$$

subject to system dynamic equation

$$\frac{\mathrm{d}}{\mathrm{d}t}\mathbf{x} = \frac{\mathrm{d}}{\mathrm{d}t}\begin{pmatrix}\Delta s\\ \Delta v\end{pmatrix} = \begin{pmatrix}\Delta v\\ u_l - u\end{pmatrix} = \mathbf{f}(\mathbf{x},\mathbf{u}) \tag{2}$$

and admissible constraints of control

$$\mathbf{u}(t) \in \mathcal{U}, \forall t \geq 0 \tag{3}$$

and initial condition:

$$\mathbf{x}(0) = \mathbf{x}_0 \tag{4}$$

In Eq. (1), J denotes the cost functional to be minimized. $\mathcal{L}$ denotes the running cost and T_p denotes the prediction horizon. u_l denotes the acceleration of the predecessor.

The running cost function is specified as:

$$\mathcal{L} = \begin{cases} \underbrace{\frac{c_1}{s}\Delta v^2 \cdot \Theta(-\Delta v)}_{\text{safety}} + \underbrace{c_2(s_d - s)^2}_{\text{efficiency}} + \underbrace{\frac{1}{2}u^2}_{\text{comfort}} & \text{if } s \leq s_f \\ \underbrace{c_3(v_0 - v)^2}_{\text{efficiency}} + \underbrace{\frac{1}{2}u^2}_{\text{comfort}} & \text{if } s > s_f \end{cases} \tag{5}$$

where $s_f = v_0 t_{d,m} + s_0$ is the gap threshold distinguishing cruising mode ($s > s_f$) from following mode ($s \leq s_f$). The gap threshold is determined by a user-defined maximum desired time gap $t_{d,m}$ at following mode, the desired speed v_0, and the minimum gap between vehicles at standstill conditions s_0. Θ is the Heaviside function, ensuing that the safety cost only occurs when approaching the preceding vehicle. s_d is the desired gap, which is determined by the current speed and a desired time gap:

$$s_d = v(t) \cdot t_d(s) + s_0 \tag{6}$$

where $t_d = t_d(s)$ is desired time gap and is dependent on traffic conditions:

$$t_d = t_{d,0} + \frac{s}{s_f}(t_{d,m} - t_{d,0}) \tag{7}$$

with $t_{d,0}$ denoting the minimum desired time gap at following mode. Equations (6, 7) show that the CFC controller employs a *variable time gap* policy, i.e. it aims to keep larger time gaps to the predecessor at loose traffic conditions (or larger gaps) and smaller time gaps when vice versa. When $t_{d,0} = t_{d,m}$, the variable time gap formulation relaxes to the constant time gap policy.

The running cost function (5) contains multiple criteria of safety, efficiency and comfort. An efficient numerical scheme based on Pontryagin's Principle is used to solve the optimal control problem (*18*).

For a *decentralized* implementation of the algorithm, each CFC vehicle solves its own optimal control problem and generates its optimal acceleration sequence. Only the first part of the sequence is implemented to updated the system state, until the optimal accelerations are recalculated after each vehicle control cycle (*7*). It is assumed that the lane-changing decisions of CFC vehicles are made and the lateral maneuvers of CFC vehicles are executed by human drivers.

In-vehicle Actuation of Traffic Control Signal

Under the connected control paradigm, intelligent vehicles serve as actuators for the traffic controller. The DSRC communication unit at each VSL gantry broadcasts the speed limit to CFC vehicles with a communication range of 200 meters. When a CFC vehicle receive the speed limit, the CFC controller changes the parameter of desired speed v_0 according to the speed limit of the freeway section the vehicle is traveling on. This entails full compliance of CFC vehicles with speed limits. The optimal acceleration is adaptively computed based on minimizing the original cost function (1,5) with *variable desired speeds*.

Although we only test the in-vehicle actuation of VSL in this study, there are multiple ways to connect the traffic controller to vehicle controllers, such as recommending route, lane choices, headways to IVs (*1*).

Implementation in Traffic Simulation

In general, the CFC algorithm can be implemented in any microscopic traffic simulator with open interface by replacing the original car-following algorithm. We implemented the CFC algorithm in an open-source microscopic traffic simulator named MOTUS (*19*). Among many other features, the MOTUS model generates realistic shock wave patterns and resembles multilane traffic flow characteristics at macroscopic level. For details of the models, we refer to (*19*).

The VSL control algorithm is implemented in Matlab. At each update of the VSL controller, with a sampling rate of 30 seconds, the VSL controller communicates with MOTUS to get the loop detector measurements along the freeway and returns the VSL control signals to the VSL gantries, resembling the cabled communication between road infrastructure (including loop detectors and VSL gantries) and traffic control centers. The loop detectors and VSL gantries are modeled in MOTUS. The communication between VSL gantries and CFC controllers are also modeled in MOTUS, and human drivers are assumed to react to the VSL gantries 150 meters upstream of each gantry.

EXPERIMENTAL DESIGN

To prove the workings and potential benefits of the connected VSL control system with CFC vehicles, simulation experiments are carried out at a bottleneck which causes stop-and-go waves if the VSL controller does not intervene. The experimental design is presented in this section.

Bottleneck and Simulation Setup

The study focuses on stop-and-go waves. Hence, the simulation is set up in analogy to a long freeway stretch where the stop-and-go wave is the major type of jams. The road network is a two-lane freeway of 14 km, with a demand of 1900 veh/h on each lane. Loop detectors are placed every 250 meters on each lane along the freeway, collecting flow and time mean speed every 30 seconds.

A bottleneck is created by temporal change of speed limits on VSL gantries on parts of the freeway. The speed limits are activated for 2 minutes, with speed values of 80 km/h, 60 km/h and 40 km/h displayed at the location of 11 km, 11.5 km and 12 km respectively.

Parameters for IDM+ in MOTUS are chosen based on the face validation on the resultant capacity drop and jam propagation characteristics, as we will show in the ensuing. We choose the same desired time gap setting of $t_{d,0} = t_{d,m} = 1.3s$ for CFC systems as for human drivers to facilitate cross-comparison of the control effects in different scenarios.

Deployment Scenarios

The variables to be tested are whether to use VSL control and the penetration rate of CFC vehicles in traffic (5%, 10%, 50%, 100%). Together with the reference scenario with 100% human drivers, this amounts to 10 simulation scenarios:

- Scenario 1 with 100% human drivers and without VSL control
- Scenario 2 with 5% CFC systems and without VSL control
- Scenario 3 with 10% CFC systems and without VSL control
- Scenario 4 with 50% CFC systems and without VSL control
- Scenario 5 with 100% CFC systems and without VSL control
- Scenario 6 with 100% human drivers and with VSL control
- Scenario 7 with 5% CFC systems and with VSL control
- Scenario 8 with 10% CFC systems and with VSL control
- Scenario 9 with 50% CFC systems and with VSL control
- Scenario 10 with 100% CFC systems and with VSL control

We conduct 10 simulation runs for each scenario.

Assessment Indicators

Total time spent (TTS) in network is the main indicator for assessing traffic efficiency. TTS is calculated from the vehicle trajectories of the simulation as:

$$\text{TTS} = \sum_{n=1}^{N_{\text{veh}}} \text{ts}_n \tag{8}$$

where ts_n denotes the time spent in the network for vehicle n and N_{veh} denotes the total number of vehicles generated in the network during the simulation period.

Extensions of the TTS indicator are included to evaluate the relative changes in traffic efficiency, which are gains in TTS of scenarios 6 - 10 with reference to scenario 1, gains in TTS in scenarios 7 - 10 with reference to scenario 6 of VSL control with 100% human-driven vehicles, and gains in TTS in scenarios 7 - 10 with respect to scenarios 2 - 5 respectively.

The number (#) of detected jams and the number of resolved jams are included, which reflect the effectiveness of the connected control paradigm in resolving shock waves, and the number (#) and location of new jams triggered by SPECIALIST is used to assess the change in flow stability property due to VSL control. Numbers of (detected, resolved and new) jams are summed over ten simulation runs, while other indicators are averaged over ten simulation runs in each scenario.

The spatio-temporal size of the VSL control scheme, A_{VSL} in $km \cdot min$ is used to assess the control effort. The speed $V_{[4]}$ and density $K_{[4]}$ of state 4 , and flow $Q_{[5]}$ of state 5 are used to assess the changes in traffic state with different penetration rate of CFC vehicles. VSL control scheme size, speed and density of state 4 and flow of state 5 are calculated by extracting different states in the VSL control scheme with loop detector data.

For sustainability indicators, we focus on average fuel consumption (AFC) rate per vehicle per 100 km. To this end, a modal fuel consumption model in (*20*) is employed. This model estimates instantaneous fuel consumption rate of vehicle n, Ft_n as a function of vehicle speed v_n and acceleration a_n:

$$\text{Ft}_n = \begin{cases} \sum_0^3 b_j v_n^j + c_1 v_n a_n + c_2 v_n a_n^2 & \text{if } a_n \geq 0 \\ \sum_0^3 b_j v_n^j + c_1 v_n a_n & \text{if } a_n < 0 \end{cases} \tag{9}$$

where b_j and c_j are model parameters. The AFC is calculated by dividing total fuel consumption by the total distance traveled of all vehicles in the network.

Apart from the indicators, spatio-temporal contour plots of flow and speed in uncontrolled scenarios (1-5) and controlled scenarios (6-10). The contour plots in controlled scenarios are coupled with VSL control scheme to visualize the control effects of the connected traffic control system.

FLOW CHARACTERISTICS OF UNCONTROLLED SCENARIOS

In this section, we summarize the flow characteristics of uncontrolled scenarios (1 - 5) (*7*), which is necessary to understand the working and effectiveness of the connected traffic control system.

Reference Human-driven Vehicular Flow (Scenario 1)

Figure 3(a)(b) show the spatio-temporal evolution of flow and time mean speed per lane on the simulated freeway collected from loop detectors. The speed limits cause vehicles in the bottleneck area to slow down, increasing the density in and limiting the outflow from the bottleneck area. Directly after the release of the speed limits, the desired speeds of vehicles in the bottleneck switch back to 120 km/h. The vehicles in the bottleneck with high density start to accelerate consequently, leading to a high flow and high speed state propagate downstream, as shown in Figure 3(a)(b). Traffic flow theorists have shown that the high density state with high flow is not stable (*21*, *22*). After a while, traffic breaks down with speeds degrading gradually, which leads to a persistent shock wave propagating backwards against the driving direction (*7*). The outflow from the jam is significantly lower than the average inflow and consequently the size of the jam increases with the course of time.

Changes in Flow Characteristics with CFC Vehicles (Scenarios 2 - 5)

There are several differences that need special attention regarding the traffic dynamics in scenarios with CFC systems compared to the reference case (*7*). First, CFC systems increase traffic efficiency. The average TTS in the network and jam sizes in scenarios 2-5 are much smaller than the reference scenario. The TTS decreases from 562.8 veh·h to 477.4 veh·h in scenario 2 and to similar values in scenarios 3 and 4. The TTS is reduced to only 443.8 veh·h when all vehicles are controlled by the CFC system, as shown in Table 2. The outflow from jams in scenarios 2 is higher than that of the reference scenario, but still lower than the inflow. Hence the capacity drop remains in scenario 2, as shown in Figure 3(c)(d). When the penetration rate increases to 10% and higher, the outflow increases more or less to the value of the inflow, resulting in shock waves with more or less constant sizes, as we can see from Figure 3(f)(h)(j).

Although the size and period of the jams are different, they all propagate in the upstream direction after the start of the bottleneck. However, unlike the reference case where the jam head propagates upstream with a *constant characteristic* velocity, the jam propagation velocity differs scenarios with CFC vehicles, as shown in Figure 3. In scenario 2, the jam head propagates faster than that of scenario 1 while in scenario 3, 4 and 5, the jam heads propagate slower than in scenario 1. In scenario 5 as shown in Figure 3(j), the shock wave first propagates upstream from 17 minutes to about 25 minutes, then it gradually changes its velocity and stays at around 9.75 km for 10 minutes and finally propagates in the *reversed* direction. After a few minutes the jam dissolves when propagating in the downstream direction. The change in jam propagation velocity is quite robust across simulation runs.

It is noteworthy that several waves propagating in the downstream direction from the jam head are observed in speed contour plots in CFC scenarios, e.g. from around 40 minutes in Figure 3(d), from around 42 minutes onwards in Figure 3(f), and from around 34 minutes in Figure 3(h). This is quite different compared to the homogeneous traffic speeds downstream of the jam area in the reference scenario 1, as shown in Figure 3(b). Although these disturbances does not result in persistent waves, it does raise some concerns on the stability property at downstream area of the jam. The CFC vehicles accelerate faster and keep a smaller gap compared to human-driven vehicles when moving out of the jam area. This increases the outflow from the jam area, but it may destabilize traffic flow downstream of the jam area.

From sustainability perspectives, the reduction of the stop-and-go waves has clear benefits in reducing fuel consumption, since the accelerating and decelerating maneuvers and their duration is substantially reduced with the decreasing size of jams. As we can see from Table 2, the average spatial fuel consumption rates are reduced when CFC vehicles present in the network, and the benefits increase with the increase of penetration rate in general.

Implications for Traffic Management

The changes in flow characteristics have implications for active traffic management. Under the same strength of a bottleneck, the CFC system may stabilize the traffic flow upstream the bottleneck, which lowers the probability of traffic break down. This consequently reduces the necessity for the traffic controller to intervene. Even if the jam prevails, the more efficient outflow due to the presence of CFC systems reduces the spatial size of the jam, which is also favorable for the traffic controller since this implies less control efforts.

However, possible difficulties are also expected when controlling traffic flow with CFC systems.The resultant jam state is difficult to predict due to random distribution of controlled vehicles. Furthermore, CFC systems may destabilize traffic flow in the accelerating transition, and hence increase the risk of triggering new jams downstream of the considered jam.

The next section tests whether the advantage of the CFC system outweighs the disadvantages, and thus leads to more effective connected control system.

EFFECTIVENESS OF CONNECTED TRAFFIC CONTROL

This section discusses the effectiveness of the connected traffic control system in scenarios 6 - 10. First, the tuning of the VSL algorithm is discussed. Then the performance of the algorithm is discussed, using the assessment indicators and plots introduced in the previous section.

Tuned Variables

The tuning of the algorithm is to determine a set of parameters that is used by the VSL controller to work effectively across simulation runs. One of the changes in flow characteristics with CFC vehicles is the velocity of the downstream jam front V_{front}, which varies with different penetration rates and does not show a consistent characteristic. During the tuning of the algorithm, we use the average downstream jam front velocity over different simulation runs of uncontrolled scenarios under the same CFC penetration rate to predict the jam front velocity, as shown in Table 1. Although the VSL controller have no knowledge of the traffic composition at the specific location of the jam, this does not turn out to be problem for the workings of the SPECIALIST algorithm.

The impact study in the previous section suggests that the CFC systems tested may destabilize traffic flow in the acceleration transition. This feature increases the risk of triggering new

TABLE 1 SPECIALIST Parameter Settings for Different Scenarios

Scenario	6 (100% Human)	7 (5% CFC)	8 (10% CFC)	9 (50% CFC)	10 (100% CFC)
$V_{\max}$ (km/h)	50	50	50	50	50
V_{front} (km/h)	-12	-13	-8	-8	-8
v_{eff} (km/h)	78	75	72	72	72
$k_{\|4\|}$ (veh/km)	24	24	23	23	23
$v_{\|5\|}$ (km/h)	105	105	115	115	115
$q_{\|5\|}$ (veh/h)	1980	1980	1980	2020	2020

jams downstream of the speed control region, which is evidenced by the tuning efforts in the experiments. In many parameter settings, new jams emerge downstream of the speed limit region. As a result, the effective speed v_{eff} and target density $k_{[4]}$ in state 4 and the flow $q_{[5]}$ and speed $v_{[5]}$ of state 5 have to be chosen in such a way that the state 4 and 5 are stable and the number of new jams triggered the VSL control scheme is as low as possible. In general, decreasing the density in state 4 and state 5 reduces the number of new jams triggered by VSL.

The tuning of the SPECIALIST algorithm follows the heuristic method in (*13*). The tuned parameters for SPECIALIST algorithm are summarized in Table 1. Note that we did not optimize the control parameters during the tuning, which involves large numbers of simulation runs and consequently considerable computation efforts needed due to the receding horizon algorithms of CFC controllers. Nevertheless, as we will show in the ensuing, the chosen parameter settings already prove the feasibility of the connected control paradigm and show its potential benefits in improving traffic operations and sustainability.

Performance of the Integrated Control Paradigm

Despite the difficulties we envisaged on traffic management with CFC vehicles due to the changed flow characteristics, our simulation experiments show that without changing the SPECIALIST algorithm, the connected VSL control works well and solves the resultant shock waves efficiently. Table 2 shows the number of detected jams and the number of jams solved by the connected VSL control. In the tested scenarios with CFC systems, all the detected jams are resolved within the spatio-temporal region of the simulation, i.e. around 10 km in space and 40 minutes in time for VSL control. Figure 4 shows typical contour plots of flow and density in different scenarios where jams are resolved successfully. One out of 10 jams in scenario 1 with 100% human drivers is not resolved eventually, which is shown in Figure 5(a)(b).

New jams are triggered by the VSL control scheme in scenario 7, 9 and 10, as shown in Figure 5(c)-(h). All the new jams are observed downstream of the speed limit region, which is in accordance with our expectations based on the changed flow characteristics. The CFC vehicles destabilizes traffic flow in the accelerating phase after the release of speed limit, which deteriorates the VSL controller performance to a certain extent.

Resolving moving jams has clear benefits in improving traffic efficiency. Compared to the reference scenario 1 without VSL control, applying SPECIALIST in the 100% human drivers scenario already brings a saving of 87.7 veh·h in the simulation period. With 5% CFC vehicles in traffic, the gain in TTS increases to 119 veh·h in scenario 7, and is slightly higher in scenarios 8, 9

and 10.

When comparing to scenario 6 with 100% human drivers, the benefits of the connected VSL control are considerable. The average TTS gain in scenario 7 with 5% CFC vehicles is 31.4 veh·h, and is higher in scenarios 8, 9 and 10 with more CFC vehicles in traffic. Even comparing to the scenarios with the same CFC penetration rate, the benefits of the connected VSL control in traffic efficiency are clear. The average TTS gain of in scenario 7 is 33.8 veh·h compared to scenario 2. This gain is decreasing with increasing penetrate rate of CFC vehicles, due to the mitigated *capacity drop* phenomenon with more CFC vehicles in traffic. Nevertheless, a slight gain of 2.1 veh·h is still observed of VSL control with 100% CFC compared to the uncontrolled scenario 5, where the jam size is already very small.

The spatio-temporal size of the VSL scheme decreases with the increase of CFC penetration rate. This is explained by the reduced jam size with more CFC vehicles in traffic. The reduced jam size implies less control efforts, i.e. less traffic are limited to enter the jam region to resolve the shock wave.

The average speed in state 4 gives an indication of the compliance rate of the traffic under speed limits. At low penetration rates of 5% and 10%, the traffic speeds in state 4 are slightly lower than those in scenario 6. When the penetration rate of CFC vehicles increases to 50%, the average speed decreases substantially to 67.7 km/h. With 100% CFC vehicles, the average speed in area 4 is 59.9 km/h, due to the full compliance of CFC vehicles.

The average flow rate in state 5 reflects how efficient the resultant flow is after the release of speed limits. It is clear that flow rates in state 5 in all controlled scenarios are higher than the fixed demand of 1900 veh/h, which is essential to resolve stop-and-go waves. It is interesting to see that with low CFC vehicle penetration rates of 5% and 10%, the resultant flow rates of state 5 are much higher than in the 50% and 100% case. This is explained by the mitigated capacity drop phenomenon due to CFC vehicles. The mechanism that slowing down vehicles to get more efficient flow works still with high penetration rate of CFC vehicles, however, the increase in outflow is less significant compared to scenarios where more human-driven vehicles present in traffic.

From sustainability perspectives, the benefits of connected traffic control are clear. In all controlled scenarios (6 - 10), the average spatial fuel consumption rates are lower than their uncontrolled counterparts with the same traffic compositions (scenarios 1 - 5). Furthermore, for all controlled scenarios with CFC systems in traffic (scenarios 7 - 10), the average spatial fuel consumption rates are lower than the controlled scenario with 100% human drivers (scenario 6).

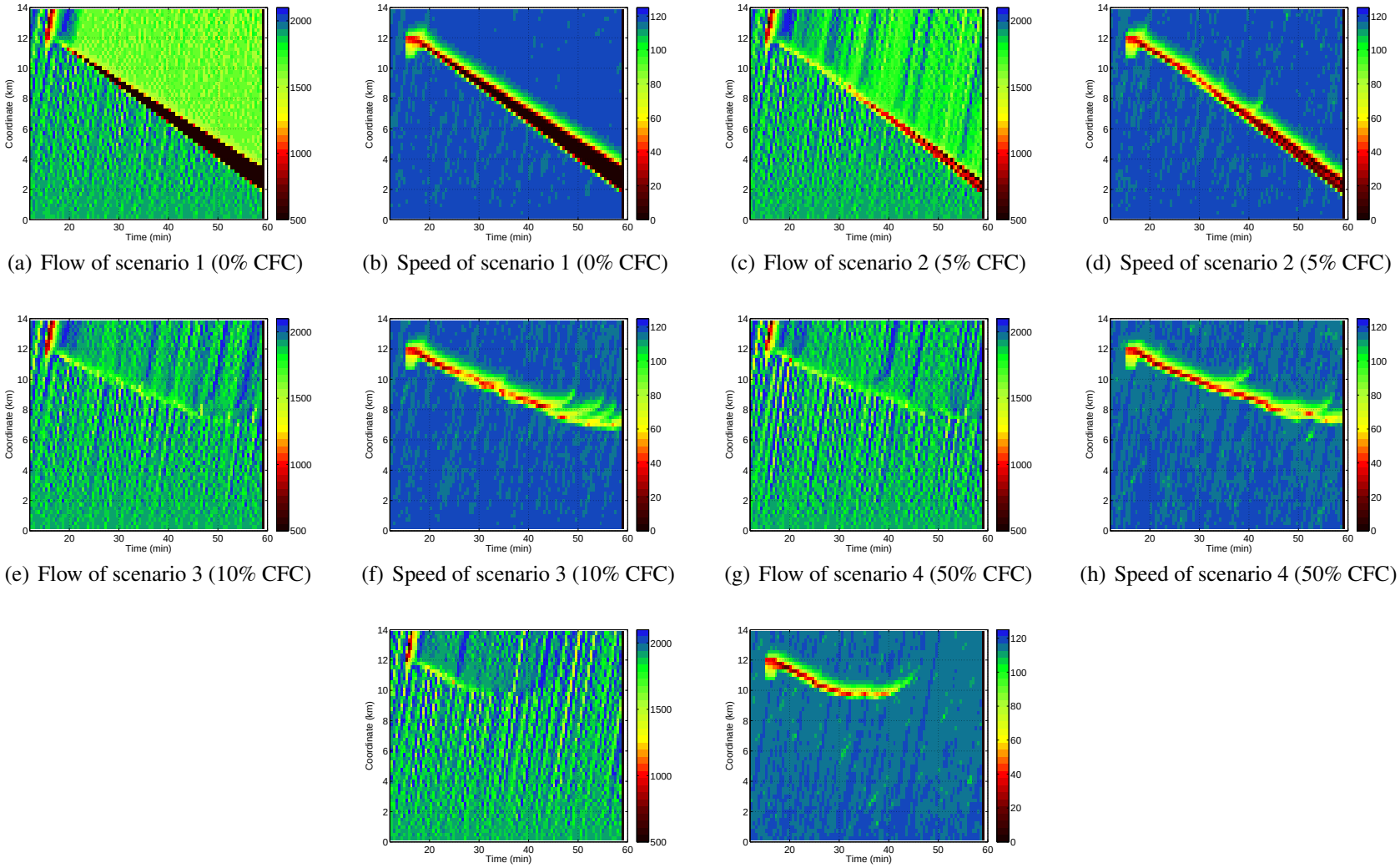

(a) Flow of scenario 1 (0% CFC)
(b) Speed of scenario 1 (0% CFC)
(c) Flow of scenario 2 (5% CFC)
(d) Speed of scenario 2 (5% CFC)
(e) Flow of scenario 3 (10% CFC)
(f) Speed of scenario 3 (10% CFC)
(g) Flow of scenario 4 (50% CFC)
(h) Speed of scenario 4 (50% CFC)
(i) Flow of scenario 5 (100% CFC)
(j) Speed of scenario 5 (100% CFC)

FIGURE 3 Flow and speed contour plots of scenarios 1 - 5. Driving direction is from bottom to top in each figure.

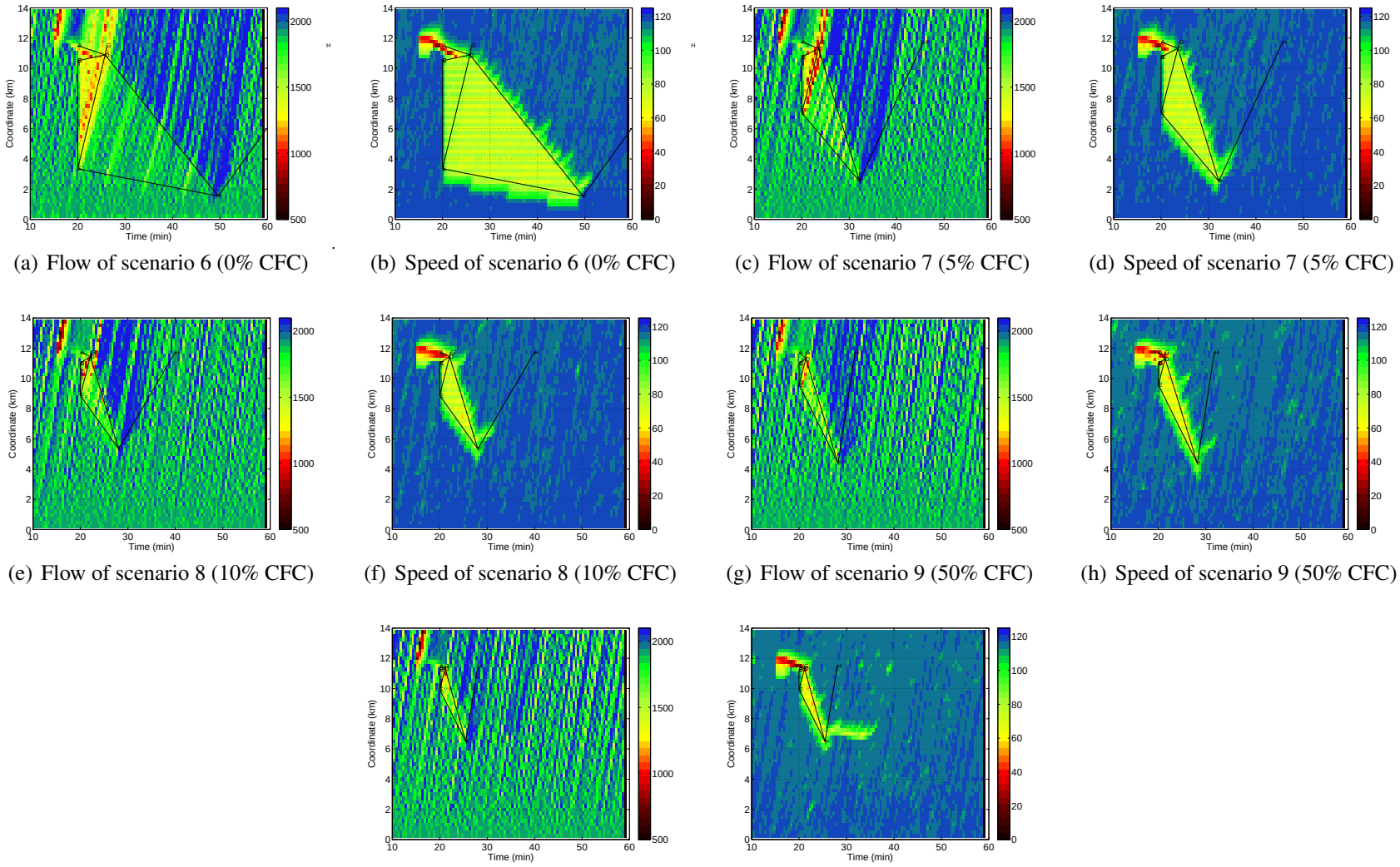

(a) Flow of scenario 6 (0% CFC)
(b) Speed of scenario 6 (0% CFC)
(c) Flow of scenario 7 (5% CFC)
(d) Speed of scenario 7 (5% CFC)
(e) Flow of scenario 8 (10% CFC)
(f) Speed of scenario 8 (10% CFC)
(g) Flow of scenario 9 (50% CFC)
(h) Speed of scenario 9 (50% CFC)
(i) Flow of scenario 10 (100% CFC)
(j) Speed of scenario 10 (100% CFC)

FIGURE 4 Flow and speed contour plots of scenarios 6 - 10. Driving direction is from bottom to top in each figure.

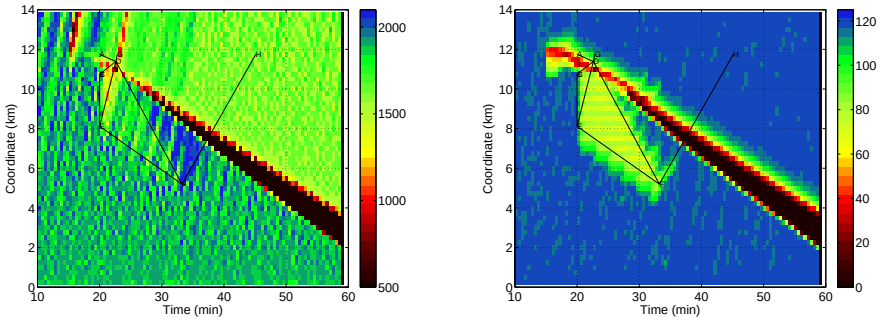

(a) Flow of scenario 6 with the unresolved jam

(b) Speed of scenario 6 with the unresolved jam

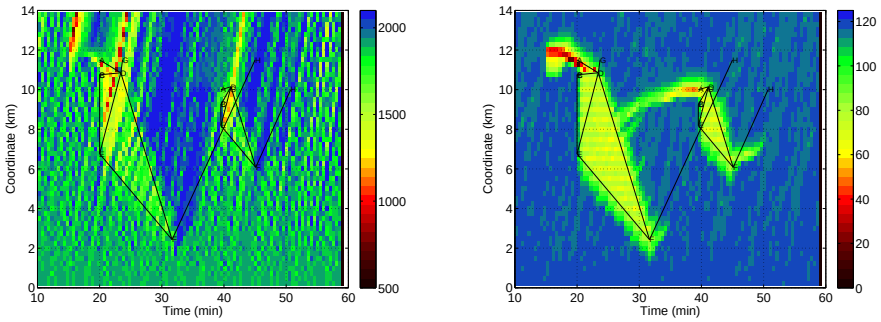

(c) Flow of scenario 7 with the new jam

(d) Speed of scenario 7 with the new jam

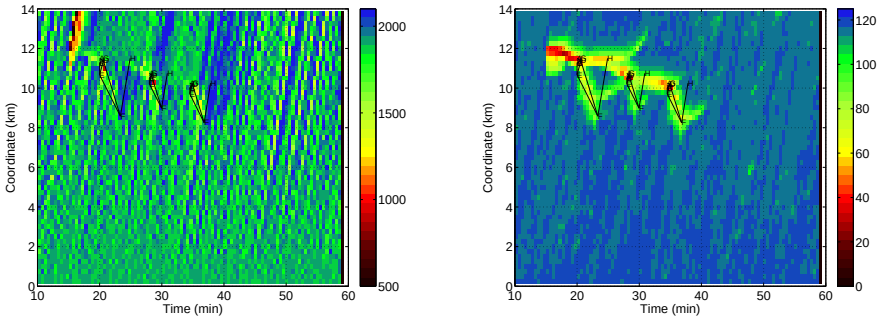

(e) Flow of scenario 9 with two new jams

(f) Speed of scenario 9 with two new jams

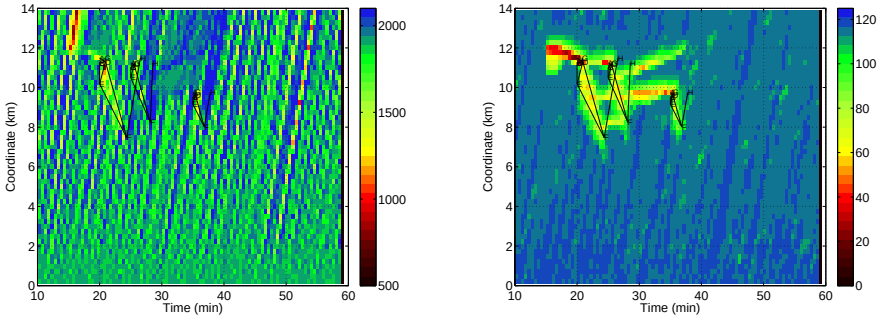

(g) Flow of scenario 10 with two new jams

(h) Speed of scenario 10 with two new jams

FIGURE 5 Spatio-temporal plots of flow and speed in scenarios with the unresolved jam and new jams triggered by VSL control.

TABLE 2 Indicators for Different Scenarios

Scenarios	VSL	# detected jams *	# resolved jams	# and location of new jams	TTS (veh·h)	TTS gain to Scen. 1 (veh·h)	TTS gain to Scen. 6 (veh·h)	TTS gain to Scen. with same penetrate rate (veh·h)	A_{VSL} (km·min)	V_4 (km/h)	Q_5 (veh/h)	AFC (l/100/km)
1 (100% Human)	off	–	–	–	562.8	–	–	–	–	–	–	4.07
2 (5% CFC)	off	–	–	–	477.4	–	–	–	–	–	–	3.91
3 (10% CFC)	off	–	–	–	453.8	–	–	–	–	–	–	3.81
4 (50% CFC)	off	–	–	–	454.4	–	–	–	–	–	–	3.84
5 (100% CFC)	off	–	–	–	443.8	–	–	–	–	–	–	3.69
6 (100% Human)	on	10	9	0	475.0	87.8	–	–	82.0	75.2	1942	3.91
7 (5% CFC)	on	11	11	1,ds**	443.6	119.2	31.4	33.8	22.4	73.3	2000	3.65
8 (10%CFC)	on	10	10	0	439.2	123.6	35.8	14.6	10.2	73.5	1982	3.61
9 (50% CFC)	on	12	12	2, ds	440.0	122.8	35.0	14.4	3.7	67.7	1945	3.62
10 (100% CFC)	on	12	12	2, ds	441.7	121.1	33.3	2.1	2.7	59.9	1926	3.65

*: # of detected, resolved and new jams are summed over ten simulation runs in each scenario, while other indicators are averaged over ten simulation runs.
**: ds stands for downstream of the VSL control region.

CONCLUSIONS

In this study, we performed a proof-of-concept study that connecting traffic control system with vehicle control system via V2I communication and investigate the changes in flow characteristics and control effectiveness with different penetration rates of IVs. Simulation results show that CFC systems improve traffic efficiency and changes flow characteristics substantially. Despite the significant changes in flow characteristics, the connected control concept works without fundamentally changing the VSL algorithm (SPECIALIST algorithm) and resolves stop-and-go waves successfully in all the test cases with CFC vehicles in traffic.

Results also show improvements in control effectiveness of the connected VSL and CFC control system, i.e. more than 80 veh·h of TTS in the network is reduced compared to uncontrolled scenarios with 100% human drivers and more than 30 veh·h of TTS is reduced to controlled scenarios with 100% human drivers. The improvement is a result of the combination of smaller capacity drop problem due to the presence of CFC vehicles and the better compliance of the CFC vehicles to the VSL control commands.

It should be noticed that the fact that the flow characteristics after the release of the speed limits (state 5 in SPECIALIST) are different with CFC vehicles in traffic, i.e. the instability triggered new jam in state 5 for scenarios with CFC vehicles and the decreasing flow rates in state 5 with the increasing penetrate rate of CFC vehicles. As SPECIALIST is originally designed for human-driven vehicular flow, re-design of the algorithm taking into account the fundamental changes in traffic flow dynamics at bottlenecks and under variable speed limits may be even more beneficial.

Apart from the in-vehicle actuation of variable speed limits concept, connecting ramp metering, route guidance or dynamic lane allocation system with intelligent vehicles are other new concepts in active traffic management. Our work sets up an example for operationalizing and testing these control concepts in the future. In addition, we only consider full compliance of the intelligent vehicle to traffic control commands. For driver assistance systems, human factors play an important role. Including these aspects is important to understand the interaction between drivers and intelligent vehicle systems and their impact on traffic operations. This leaves another interesting topic for future research.

ACKNOWLEDGMENT

This research is sponsored by Royal Dutch Shell under the project “Sustainability Perspectives of Cooperative Systems”.

REFERENCES

[1] Varaiya, P. and S. E. Shladover. Sketch of an IVHS systems architecture. *Vehicle Navigation and Information Systems Conference*, Vol. 2, 1991, pp. 909–922.

[2] Tsugawa, S., S. Kato, T. Matsui, H. Naganawa, and H. Fujii. An architecture for cooperative driving of automated vehicles. *IEEE Conference on Intelligent Transportation Systems*, 2000, pp. 422–427.

[3] Alkim, T. P., H. Schuurman, and C. M. J. Tampère, Effects of external cruise control and co-operative following on highways: an analysis with the MIXIC traffic simulation model. In *Intelligent Vehicles Symposium, 2000. IV 2000. Proceedings of the IEEE*, 2000, pp. 474–479.

[4] Kovacs, A., Z. Jeftic, N. Nygren, and T. Hilgers, *CVIS Project Deliverable: D.CVIS.2.2 - Use Cases and System Requirements*, 2006.

[5] Shladover, S. E., *Recent International Activity in Cooperative VehicleHighway Automation Systems*. Federal Highway Administration, USDOT, 2012.

[6] Monteil, J., R. Billot, D. Rey, and N.-E. E. Faouzi. Distributed and Centralized Approaches for Cooperative Road Traffic Dynamics. *Procedia - Social and Behavioral Sciences*, Vol. 48, No. 0, 2012, pp. 3198 – 3208, transport Research Arena 2012.

[7] Wang, M., *Generic Model Predictive Contorl Framework for Advanced Driver Assistance Systems*. Ph.D. thesis, Department of Transport and Planning, Delft University of Technology, 2014.

[8] Yuan, Y., J. W. C. Van Lint, R. Wilson, F. van Wageningen-Kessels, and S. Hoogendoorn. Real-Time Lagrangian Traffic State Estimator for Freeways. *Intelligent Transportation Systems, IEEE Transactions on*, Vol. 13, No. 1, 2012, pp. 59–70.

[9] Netten, B., A. Hegyi, M. Wang, W. Schakel, Y. Yuan, T. Schreiter, B. van Arem, C. van Leeuwen, and T. Alkim. Improving moving jam detection performance with V2I communication. *Proceedings of 20th World Congress on Intelligent Transport Systems*, 2013.

[10] Vinagre Diaz, J., D. Fernandez Llorca, A. Rodriguez Gonzalez, R. Quintero Minguez, A. Llamazares Llamazares, and M. Sotelo. Extended Floating Car Data System: Experimental Results and Application for a Hybrid Route Level of Service. *Intelligent Transportation Systems, IEEE Transactions on*, Vol. 13, No. 1, 2012, pp. 25–35.

[11] Ioannou, P., Y. Wang, and H. Chang, *Integrated Roadway/Adaptive Cruise Control System: Safety, Performance, Environmental and Near Term Deployment Considerations*. UCB-ITS-PRR-2007-8, University of Southern California, 2007.

[12] Hegyi, A., B. Netten, M. Wang, W. Schakel, T. Schreiter, Y. Yuan, B. van Arem, and T. Alkim, A cooperative systems based variable speed limit control algorithm against jam waves an extension of the SPECIALIST algorithm. In *Proceedings of the 16th International IEEE Conference on Intelligent Transportation Systems*. The Hague, The Netherlands, 2013, pp. 973–978.

[13] Hegyi, A. and S. P. Hoogendoorn, Dynamic speed limit control to resolve shock waves on freeways - Field test results of the SPECIALIST algorithm. In *13th IEEE International Conference on Intelligent Transportation Systems*. Madeira, Portugal, 2010, pp. 519–524.

[14] Carlson, R. C., I. Papamichail, M. Papageorgiou, and A. Messmer. Optimal mainstream traffic flow control of large-scale motorway networks. *Transportation Research Part C: Emerging Technologies*, Vol. 18, No. 2, 2010, pp. 193 – 212.

[15] Lu, X.-Y., P. Varaiya, R. Horowitz, D. Su, and S. Shladover. Novel Freeway Traffic Control with Variable Speed Limit and Coordinated Ramp Metering. *Transportation Research Record: Journal of the Transportation Research Board*, Vol. 2229, No. -1, 2011, pp. 55–65.

[16] Lighthill, M. J. and G. B. Whitham. On Kinematic Waves II: A Theory of Traffic Flow on Long Crowded Roads. *Proceedings of the Royal Society of London Series a-Mathematical and Physical Sciences*, Vol. 229, No. 1178, 1955, pp. 317–345, iSI Document Delivery No.: WU245 Times Cited: 742 Cited Reference Count: 17.

[17] Wang, M., M. Daamen, S. P. Hoogendoorn, and B. van Arem. Rolling horizon control framework for driver assistance systems. Part I: Mathematical formulation and non-cooperative systems. *Transportation Research Part C: Emerging Technologies*, Vol. 40, No. 0, 2014, pp. 271 – 289.

[18] Hoogendoorn, S. P., R. Hoogendoorn, M. Wang, and W. Daamen. Modeling Driver, Driver Support, and Cooperative Systems with Dynamic Optimal Control. *Transportation Research Record: Journal of the Transportation Research Board*, Vol. 2316, No. -1, 2012, pp. 20–30.

[19] Schakel, W. J., V. Knoop, and B. van Arem. Integrated Lane Change Model with Relaxation and Synchronization. *Transportation Research Record: Journal of the Transportation Research Board*, Vol. 2316, 2012, pp. 47–57.

[20] Akcelik, R. Efficiency and drag in the power-based model of fuel consumption. *Transportation Research Part B: Methodological*, Vol. 23, No. 5, 1989, pp. 376 – 385.

[21] Treiber, M. and A. Kesting. *Traffic Flow Dynamics*. Springer, 2013.

[22] Wilson, R. E. Mechanisms for spatio-temporal pattern formation in highway traffic models. *Philosophical Transactions of the Royal Society A: Mathematical, Physical and Engineering Sciences*, Vol. 366, No. 1872, 2008, pp. 2017–2032.